Interlayer magnetic coupling in epitaxial NiFe/Ru/NiFe trilayers

2004 J. Phys.: Condens. Matter 16 7163

(http://iopscience.iop.org/0953-8984/16/39/047)

INSTITUTE OF PHYSICS PUBLISHING JOURNAL OF PHYSICS: CONDENSED MATTER

J. Phys.: Condens. Matter **16** (2004) 7163–7168 PII: S0953-8984(04)82970-9

Interlayer magnetic coupling in epitaxial NiFe/Ru/NiFe trilayers

I F Lee[1], J C Jan[1], J W Chiou[1], H M Tsai[1], C W Bao[1], W F Pong[1,6], M-H Tsai[2], H H Hsieh[3], T Y Hou[3], H-J Lin[3], L Y Jang[3], H H Hung[3], W C Chen[4,5] and J C A Huang[4,5]

[1] Department of Physics, Tamkang University, Tamsui 251, Taiwan
[2] Department of Physics, National Sun Yat-Sen University, Kaohsiung 804, Taiwan
[3] National Synchrotron Radiation Research Center, Hsinchu 300, Taiwan
[4] Department of Physics, National Cheng Kung University, Tainan 701, Taiwan
[5] Department of Applied Physics, National University of Kaohsiung, Kaohsiung 811, Taiwan

E-mail: wfpong@mail.tku.edu.tw

Received 7 July 2004, in final form 9 August 2004
Published 17 September 2004
Online at stacks.iop.org/JPhysCM/16/7163
doi:10.1088/0953-8984/16/39/047

Abstract

Ni and Fe $L_{3,2}$-edge x-ray magnetic circular dichroism (XMCD) and Ru L_3-edge x-ray absorption spectroscopy (XAS) measurements have been performed for Py/Ru(t_{Ru})/Py (Py = $Ni_{80}Fe_{20}$) trilayers with t_{Ru} = 15, 20, 25, and 30 Å. The XMCD asymmetry ratios in the Ni and Fe L_3-edge spectra show a dip at t_{Ru} = 20 Å. At this particular thickness, the magneto-optical Kerr effect hysteresis loop measurements show that the Py–Py magnetic coupling is ferromagnetic, which differs from the antiferromagnetic couplings for other Ru spacer layer thickness. The Ru L_3-edge XAS results show that the intensity of the white-line feature decreases rapidly as a quadratic function of t_{Ru} within the range between 15 and 30 Å.

1. Introduction

The oscillatory magnetic coupling between two ferromagnetic (FM) metal layers with an antiferromagnetic (AFM) or non-magnetic metal spacer layer has drawn increasing research interest [1–3]. Magnetization measurements for a variety of transition-metal (TM) spacers sandwiched between two FM layers performed by Parkin [4] revealed that the oscillatory behaviour and the AFM coupling are generally observed for most TM spacers. The exchange couplings of these systems are commonly interpreted by the Ruderman–Kittel–Kasuya–Yosida (RKKY) model [5]. Within the RKKY model, the oscillatory period is related to the inverse of the length of the wavevectors at the Fermi surface and should depend on the details of the Fermi

[6] Author to whom any correspondence should be addressed.

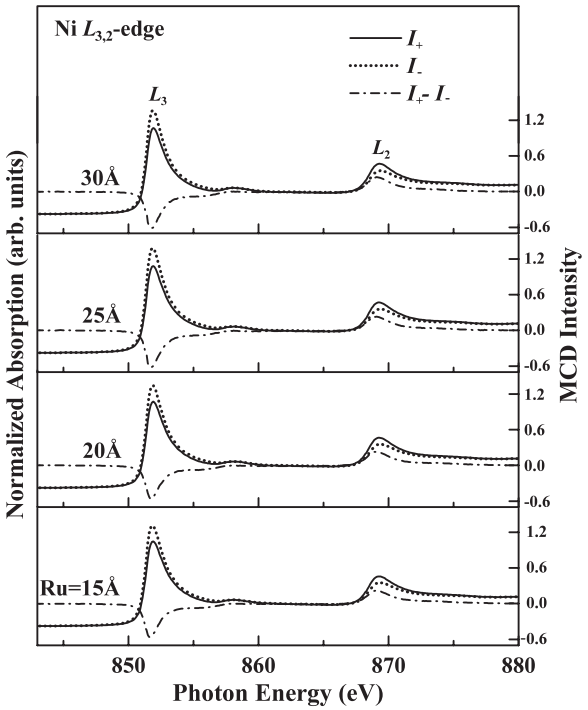

Figure 1. Normalized Ni $L_{3,2}$-edge XAS and XMCD spectra of the Py/Ru(t_{Ru})/Py trilayers with $t_{Ru} = 15$, 20, 25, and 30 Å.

surface topology of the spacer metal [1]. Previous x-ray magnetic circular dichroism (XMCD) and x-ray absorption spectroscopy (XAS) studies [6] have investigated the dependence of the element-specific magnetic properties of the Py/Cr/Py trilayers on thickness of the Cr layer, and found a correlation between the magnetic transition and the structural transition of the Cr spacer. Here, we have extended the study to the interlayer magnetic couplings of the epitaxial Py/Ru/Py trilayer for various Ru-layer thicknesses by Ni and Fe $L_{3,2}$-edge XMCD and Ru L_3-edge XAS measurements.

2. Experimental details

XMCD and XAS spectra were measured at the National Synchrotron Radiation Research Centre in Hsinchu, Taiwan, operating with an electron energy of 1.5 GeV and a maximum stored current of 200 mA. The XMCD spectra of all samples were obtained from the Dragon beamline. Using the electron yield method for the Ni and Fe $L_{3,2}$-edge the photon energy resolution was better than 0.3 eV over the measured energy range. An alternating magnetic field of 100 Oe was applied parallel to the surface of the sample, and the grazing angle of the incident light was fixed at 30° from the sample's surface. The Ru L_3-edge XAS spectra were obtained from the BL15B beamline using the fluorescence yield method. The molecular beam epitaxy grown $Py(111)_{50\ Å}$/Ru(0001)/$Py(111)_{50\ Å}$ trilayer structure with a stair-shaped Ru spacer layer was deposited at 150 °C on the Pt seeding layer on the $Al_2O_3(11\bar{2}0)$ substrate. The stair-shaped Ru layer has four 15, 20, 25, and 30 Å high (or thick) steps, which allows investigation of the dependence of the Py–Py magnetic coupling on the thickness of the Ru layer under the

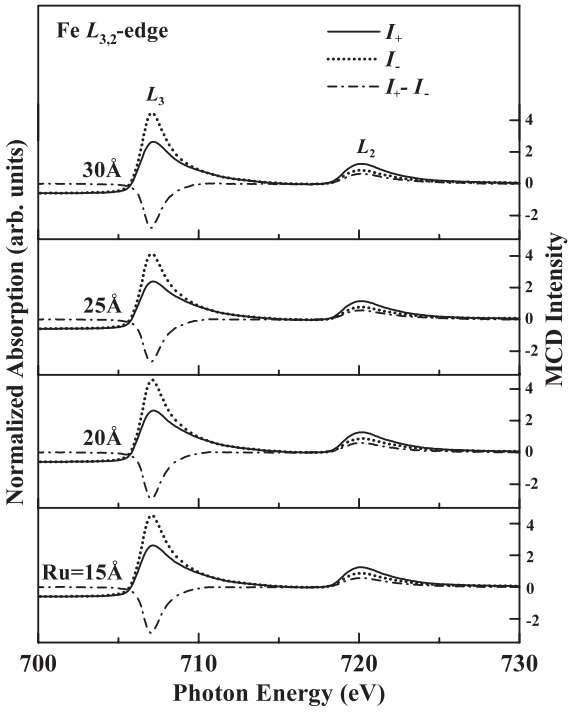

Figure 2. Normalized Fe $L_{3,2}$-edge XAS and XMCD spectra of the Py/Ru(t_{Ru})/Py trilayers with $t_{Ru} = 15$, 20, 25, and 30 Å.

same sample preparation conditions. A thin capping Pt layer (∼10 Å) was also deposited on the top of the sample to prevent oxidation problems. The details of the preparation and characterization of the samples have been presented elsewhere [7].

3. Results and discussion

Figures 1 and 2 display, respectively, the normalized Ni and Fe $L_{3,2}$-edge XAS and XMCD (i.e. $I_+ - I_-$) spectra of the Py/Ru(t_{Ru})/Py trilayers with $t_{Ru} = 15$, 20, 25, and 30 Å. I_+ (I_-) refers to the absorption spectrum obtained by projecting the spin of the incident photons parallel (antiparallel) to the spin direction of the Ni and Fe 3d majority-spin electrons. The Ni and Fe $L_{3,2}$-edge XAS and XMCD spectra also exhibit similar features to those of the Py/Cr(t_{Cr})/Py trilayers reported previously [6].

Figure 3 shows the Ni and Fe L_3-edge XMCD asymmetry ratios [6, 8] (or XMCD to XAS ratio [9, 10]), $(I_+ - I_-/I_+ + I_-)$, versus the thickness of the Ru layer. If the 3d-orbital occupation number, n_{3d}, can be accurately determined from the integrated intensities of Fe and Ni L_3-edge XAS features, which reflect the total 3d unoccupied states, in conjunction with the XMCD asymmetry ratio orbital and spin magnetic moments can be determined by *sum rules* [9, 11]. However, we found that due to difficulties with the background subtraction the application of sum rules in the present system is not reliable because the magnetic moments obtained were unreasonable compared with those of Fe and Ni. Thus, in this study we have used the variation of the L_3-edge XMCD asymmetry ratio to approximately represent the variation of the magnetic moments of Ni and Fe atoms in the NiFe alloys. The XMCD asymmetry ratios in

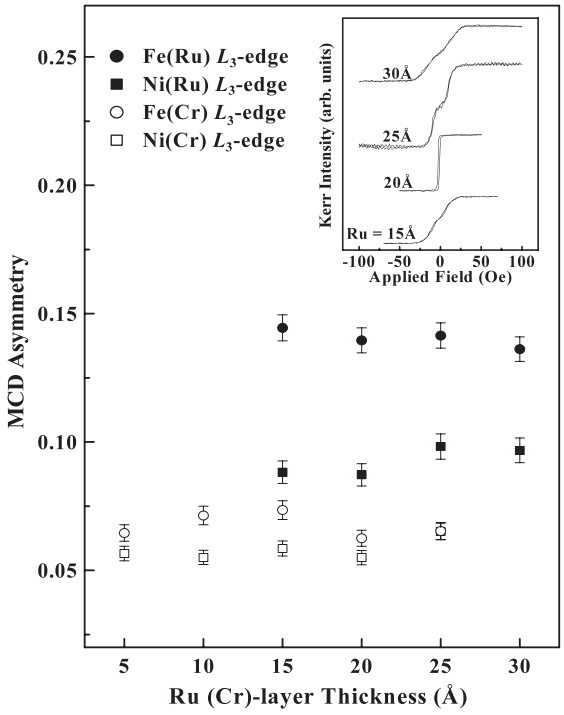

Figure 3. Ni and Fe L_3-edge XMCD asymmetry ratios versus the thickness of the Ru(Cr) layer. The inset plots MOKE hysteresis loops.

the Ni and Fe L_3-edge spectra were integrated between 847 and 860 eV and between 700 and 716 eV, respectively. As shown in figure 3, the moment of the Fe 3d states exceeds that of Ni in the Py/Ru(t_{Ru})/Py trilayers. This is because the Fe atom has a larger magnetic moment than the Ni atom. The variations of the XMCD asymmetry ratios for Fe and Ni L_3-edge spectra in the Py/Ru(t_{Ru})/Py trilayers are similar. The XMCD asymmetry ratios for both the Ni and Fe L_3-edge spectra have a dip at $t_{Ru} = 20$ Å. Since these dips are marginally within the experimental errors shown in figure 3, they may not be significant. However, the magneto-optical Kerr effect (MOKE) results suggest that the dip of the Fe and Ni L_3-edge XMCD asymmetry ratios at $t_{Ru} = 20$ Å is real. At this particular thickness, the MOKE hysteresis loop measurements [7] yielded that Py–Py has an FM coupling, while Py–Py has an AFM coupling for $t_{Ru} = 15$, 25, and 30 Å as shown in the inset of figure 3.

In figure 3, Ni and Fe L_3-edge XMCD asymmetry ratios for Py/Cr/Py are also shown for comparison with those of Py/Ru/Py. The figure shows that the Fe L_3-edge XMCD asymmetry ratios are more than two times larger for the Ru spacer than for the Cr spacer. The Ni L_3-edge XMCD asymmetry ratios for the Ru spacer, though still larger, are closer to those of the Cr spacer. The Fe L_3-edge XMCD asymmetry ratios are more than two times larger for the Ru spacer than for the Cr spacer, which may be due to stronger couplings between Fe 3d and delocalized Ru 4d states as evidenced by the significant increase of the intensity of Fe L_3-edge XAS features. In contrast, the intensity of Fe L_3-edge XAS features did not have significant change for the Cr spacer [12]. The smaller influence by the spacer layer on the Ni L_3-edge XMCD asymmetry ratio is because the Ni atom has a smaller magnetic moment than the Fe atom. Another influence on the inter-FM-layer magnetic coupling by the TM spacer is the type of the magnetic coupling. For the Py/Cr/Py trilayer, the inter-FM-layer magnetic coupling is ferromagnetic when t_{Cr} is less than 20 Å and the coupling becomes antiferromagnetic when t_{Cr} is equal to and larger than 20 Å. The transition from FM to AFM coupling was correlated with

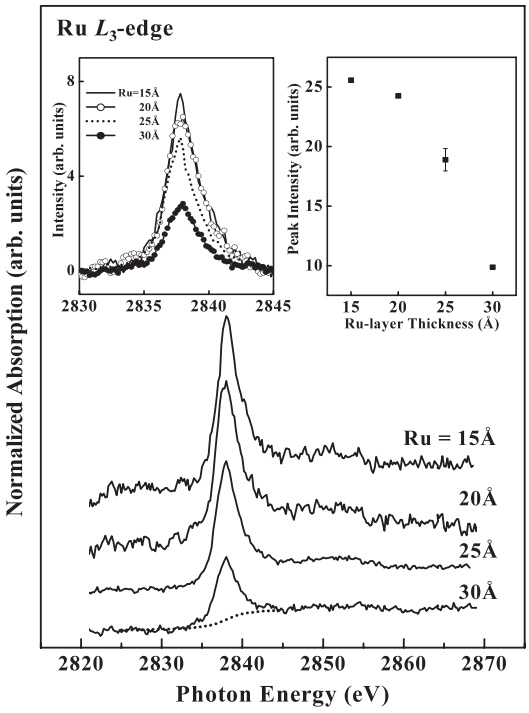

Figure 4. Normalized Ru L_3-edge XAS spectra of the Py/Ru(t_{Ru})/Py trilayers with t_{Ru} = 15, 20, 25, and 30 Å. The dashed curve represents the extrapolated background at the Ru L_3-edge. The centre of the continuum step of the arctangent function was selected at the maximum height of the white-line features. The white-line region of the Ru L_3-edge and the integrated intensities are shown in the left and right insets, respectively.

a structural transition from the strained closest packed fcc structure of the Ni-rich Py layer to the bcc structure of the bulk Cr metal [6]. As for the Py/Ru/Py trilayer, the Py–Py coupling is ferromagnetic only for the $t_{Ru} = 20$ Å sample and all other thinner and thicker samples have AFM couplings (shown in the inset of figure 3). Since the bulk Ru metal has the closest packed hexagonal structure [13], which differs from the fcc structure only in the stacking sequence along the [111] or [0001] direction, the Py/Ru/Py trilayer may not have a structural transition when t_{Ru} is increased. The MOKE hysteresis loops shown in the inset of figure 3 suggest that for t_{Ru} in the vicinity of 20 Å the Fermi level, E_F, lies near the local minimum in the Ru 4d band between its two subbands, while for $t_{Ru} < 20$ Å and $t_{Ru} > 20$ Å E_F lies in the upper and lower subbands, respectively. At $t_{Ru} = 20$ Å the contribution of itinerant Ru 5s and 5p electrons to the Py–Py magnetic coupling, which favours FM couplings, becomes important. For $t_{Ru} < 20$ Å and $t_{Ru} > 20$ Å the contribution of Ru 4d electrons dominates and the Py–Py coupling is antiferromagnetic.

The thickness dependence of E_F relative to the Ru 4d band can be inferred from the Ru L_3-edge XAS spectra of the Py/Ru(t_{Ru})/Py trilayers as shown in figure 4. The spectra have been divided by the incident intensity I_0 and then normalized to the same area in the energy range between 2857 and 2868 eV, which is a common normalization procedure for x-ray absorption spectra. It has been established that the Ru L_3-edge white-line intensity is strongly sensitive to the Ru 4d band occupation [14]. The white-line features $I(L_3)$ at the Ru L_3-edge are illustrated and their intensities integrated between 2830 and 2847 eV as a function of the

thickness of the Ru layer are plotted in the left and right insets of figure 4, respectively. $I(L_3)$ is determined by subtracting the background intensity described by an arctangent function, as indicated by the dashed curve in figure 4. Due to the limited number of data points and experimental uncertainty shown in the right inset of figure 4, the dependence of the intensity of the white-line feature on the Ru-layer thickness can be either approximately represented by an inverted parabolic or shifted exponential function. The ratio between $I(L_3)$ values for 30 and 15 Å is about 0.4. If $I(L_3)$ is directly proportional to the number of 4d holes, h_{4d}, in the Ru atom and h_{4d} is assumed to be close to that of a free Ru atom of three for the 15 Å spacer, then h_{4d} will be about unity with a $4d^9$ configuration for the Ru atoms in the 30 Å spacer, which is unlikely. $I(L_3)$ depends not only on h_{4d} but also on the dipole transition probability from Ru 2p core to unoccupied 4d states. Thus, $I(L_3)$ depends on the degree of delocalization of the 4d orbitals, which is larger for thicker Ru spacers. A larger degree of delocalization yields a smaller transition probability. Thus, the rapid drop of $I(L_3)$ with the increase of t_{Ru} may be a combined effect of the decrease of the transition probability and h_{4d}. The decrease of h_{4d} may be due to an increase of the work function that results in a charge transfer into Ru 4d orbitals from the Py layers.

4. Conclusion

In summary, this work examined the dependence of the element-specific magnetic properties of the Py/Ru/Py trilayers on the thickness of the Ru spacer layer. We found a dip in the Ni and Fe L_3-edge XMCD asymmetry ratios when the Ru-layer thickness is ∼20 Å. At this particular thickness, the MOKE hysteresis loop measurements show that the Py–Py magnetic coupling is ferromagnetic, which differs from the antiferromagnetic couplings for other Ru spacer layer thickness. The Ru L_3-edge XAS results show that the intensity of the white-line feature decreases rapidly as a quadratic function of t_{Ru} in the range between 15 and 30 Å, which may be due to the decrease of both the dipole transition probability and the density of unoccupied Ru 4d states.

Acknowledgment

The author WFP would like to thank the National Science Council of the Republic of China for financially supporting this research under contract No NSC 92-2112-M-032-025.

References

[1] Heinrich B and Bland J A C (ed) 1994 *Ultrathin Magnetic Structure* vol I and II (Berlin: Springer)
[2] Grunberg P, Schreiber R, Pang Y, Brodsky M B and Scwers H 1986 *Phys. Rev. Lett.* **57** 2442
[3] Baibich M N, Broto J M, Fert A, Nguyen Van Dau F, Petroff F, Etienne P, Creuzet G, Friederich A and Chazelas J 1988 *Phys. Rev. Lett.* **61** 2472
[4] Parkin S S P 1991 *Phys. Rev. Lett.* **67** 3598
[5] Yafet Y 1987 *Phys. Rev.* B **67** 493
[6] Lee I F, Shen M Y, Lay Y Y, Jan J C, Chiou J W, Tsai H M, Pong W F, Tsai M-H, Hsieh H H, Lin H-J, Lee J F, Ku C A and Huang J C A 2003 *Appl. Phys. Lett.* **82** 3062
[7] Huang J C A *et al* unpublished
[8] Pong W F, Chang Y K, Su M H, Tseng P K, Lin H-J, Ho G H, Tseng K L and Chen C T 1997 *Phys. Rev.* B **55** 11409
[9] Thole B T, Carra P, Sette F and van der Laan G 1992 *Phys. Rev. Lett.* **68** 1943
[10] Idzerda Y U, Tjeng L H, Lin H-J, Gutierrez C J, Meigs G and Chen C T 1993 *Phys. Rev.* B **48** 4144
[11] Carra P, Thole B T, Altarelli M and Wang X 1993 *Phys. Rev. Lett.* **70** 694
[12] Lin T, Tomaz M A, Schwickert M M and Harp G R 1998 *Phys. Rev.* B **58** 862
[13] *Periodic Table of the Elements* 1980 (Skolie, IL: Sargent-Welch Scientific Company)
[14] Sham T K, Ohta T, Yokoyama T, Kitajima Y, Funabashi M, Kosugi N and Kuroda H 1988 *J. Chem. Phys.* **88** 475